

Factors affecting the adsorption of stabilisers on to carbon black (flow micro-calorimetry and FTIR studies)

Part I *Primary phenolic antioxidants*

J. M. PEÑA, N. S. ALLEN*, M. EDGE, C. M. LIAUW, F. SANTAMARÍA
*Department of Chemistry and Materials, Manchester Metropolitan University,
Chester Street, Manchester M1 6GD, UK
E-mail: n.allen@mmu.ac.uk*

O. NOISET, B. VALANGE
Cabot Corporation, Rue Prevostchamps 78, 4860 Pepinster, Belgium

The surface activity of different types of carbon black with phenolic antioxidants is examined using flow micro-calorimetry (FMC), X-ray Photoelectron Spectroscopy (XPS) and Fourier Transform Infrared spectroscopy (FTIR). Significant differences in both the overall adsorption activity and the levels of probe adsorption are observed. Differences in behaviour between types of carbon black are evident and show that the specific surface area is not the most important factor affecting the adsorption activity, but also the chemical nature of its surface. Essentially, two factors were found to affect the behaviour of phenolic stabilisers: Phenolic hydroxyl and ester groups were found to form the strongest interactions with carbon black. Furthermore, steric hinderance of phenolic hydroxyls by alkyl groups is the main factor which influences adsorption activity. In order to characterise different carbon blacks, FTIR and XPS analysis have been used in an attempt to determine the nature of functional groups present on the surface of the carbon blacks. FTIR analysis also shows that some adsorbed antioxidants on the surface of the carbon black could be successfully detected. This provides valuable information regarding the adsorption mechanisms on to carbon black surfaces. Other techniques included thermogravimetric analysis (TGA), N₂ BET adsorption studies and Karl Fisher analysis. The latter were performed in order to determine differences in the volatile and water contents, respectively, of the carbon black samples. © 2001 Kluwer Academic Publishers

1. Introduction

The effect of carbon black surface chemistry on interactions with stabilisers in thermoplastics based formulations has not been studied in detail. However, chemical and physical interactions between carbon black surface groups and polar elastomer matrix chains were found to promote high reinforcement activity in many instances [1]. In thermoplastics, the adsorption of stabilisers onto fillers is a recognised problem that is solved by using additives which sacrificially adsorb on to the filler surfaces thereby blocking the adsorption of the stabilisers [2].

Previous studies on other varieties of filler [3] indicated that the adsorption of stabilisers is not necessarily a negative feature and this can be used to provide what can be considered as a reservoir of stabilisers.

In order to understand how the stabilisers are adsorbed and under which conditions they can be released, the interactions between carbon black and antioxi-

dants must be well understood. Flow micro-calorimetry (FMC) has proved to be a useful technique for studying the interactions between carbon black and stabilisers in this investigation [4].

However, the very complex physical structure of carbon black and the presence of numerous oxygen containing functional groups hamper attempts to obtain precise knowledge of the adsorption-desorption mechanism of stabilisers onto carbon black. The presence of impurities and adsorbed water can cause further complications in the surface analysis of carbon black.

In general, furnace blacks contain 9 mg of oxygen per 100 m² of the surface [5]. Carbon blacks may contain as much as 1.2% combined sulphur, as well as ash at a few tenths of a percent (sometimes as high as 1%). The ash consists of the salts and oxides of calcium, magnesium, sodium, and in some products

* Author to whom all correspondence should be addressed.

potassium, and accounts for the basic pH (8–10) commonly found in furnace blacks [5]. Whilst hydrogen and sulphur are distributed on the surface and in the interior of the aggregates, oxygen is almost exclusively located on the surface in the form of carbon-oxygen functional groups. These groups have been identified as carboxyl, phenols, lactones, aldehydes, ketones, quinones, hydroquinones, anhydrides and ethereal structures. Phenolic groups make up the majority of the surface oxygen content [5].

The functional groups described above (carboxylic acid, phenolic, quinone and lactones), are believed to be attached to the edges of the graphitic layers. These groups can interact with elastomers and plastics as well as others additives such as plasticisers and stabilisers. By measuring the heat of adsorption, it has been shown that the interaction with various adsorbates is strong at very low coverage and decreases sharply once the level of coverage exceeds ca. 0.2 monolayers [6]. Inverse gas chromatography (IGC) and flow microcalorimetry (FMC) have revealed significant differences in adsorption energies and entropies which are dependent on the shape of the hydrocarbon-adsorbate molecule and the structure and chemistry of the carbon black surface [7]. Polymer molecules can also be adsorbed from solution onto the carbon black, and once adsorbed they are difficult to remove. This is due both to strong bonding, at a small number of high energy sites, and to weak bonding at a large number of low energy sites, since desorption of a given polymer molecule requires simultaneous detachment of all the polymer-filler bonds [8].

Flow micro-calorimetry (FMC) has become an established method for characterising filler surfaces in terms of their surface chemistry and their interactions with surface treatments. Calorimetric techniques for the characterisation of carbons have been recently and comprehensively reviewed by Angel Menéndez [9], therefore only a very brief overview is given here. Grozeck, who has conducted numerous studies on carbon black and other carbonaceous materials [10–12], designed the Microscal FMC system used in this study. Fowkes [13, 14] also used FMC to study acid-base interactions between a variety of different probes and substrates. During the 1980's concentration detectors were added to the FMC cell outlet [13], this addition enabled the level of probe adsorption and desorption to be determined. Ashton and Rothon [15] used a UV detector and differential refractometer connected in series with the cell outlet in a study of adsorption of 3-trimethoxysilylpropyl methacrylate onto aluminium hydroxide. Data from these detectors enabled the amounts of methanol and water evolved (from self-condensation of the silane and adsorption onto the aluminum hydroxide, respectively) to be determined.

It has to be appreciated, however, the heats of adsorption determined using FMC are in actual fact the balance of enthalpies associated with several processes, some of which can be endothermic, i.e., heat of desorption of the solvent from the substrate and the heat of de-mixing of the adsorbate. The other important is-

sue for consideration is the presence of adsorbed water on the carbon black surface. This aspect has been studied extensively by Grozeck [12] who has found that water binds very strongly to the polar groups on the surface. Therefore under most circumstances the strongly adsorbed water can be considered to be a feature of a given carbon black that will affect the adsorption of a variety of probes. It can be argued that removal of the water will give a false impression of the adsorption characteristics of, for example, polymer additives on to the carbon black during processing and in the end use application of the product. In our earlier studies [3, 16] on silica filled PE we found that the adsorption data could be related to enhanced stabilisation synergy, in this study no attempt was made to dry the silica before introducing to the FMC cell.

The work described in this paper forms part of a far larger programme investigating the effect carbon black-stabiliser interactions on the thermal and UV stability of carbon black pigmented polyethylene. This study, reporting factors affecting the adsorption of phenolic stabilisers onto four carbon blacks with varying oxygen content, forms a worthwhile contribution to the huge canon of works on adsorption of molecules onto carbon black. More importantly, however, this study sheds light on filler-stabiliser interactions that can occur in carbon black filled polymers. Such interactions may have the potential, if correctly utilised and understood, to enhance the stability of such materials.

2. Experimental

2.1. Materials

The Primary hindered phenolic antioxidants investigated were Irganox 1010, Irganox 1076, Irganox 1330 and Irganox 3114 (all from Ciba, UK) and Cyanox 1790 (from Cytec). The structures of these stabilisers are shown in Fig. 1 and further details are provided in Table I. The phenolic model compounds (Fig. 2), used in order to study the effect of steric hindrance in phenolic antioxidants, were: Phenol, 2,6 Dimethyl phenol, 2,4 Di-*tert*-butyl phenol, 2-*Tert*-butyl 6-methyl phenol, Tri-*tert*-butyl phenol (all from Aldrich).

The furnace carbon blacks, CB-A, CB-B, CB-C and CB-D, were supplied by the Cabot Corporation. Their features are given in Table II. It must be pointed out these carbon blacks were not treated with any form of binder. Therefore the results reported reflect only the chemical nature and structure of the blacks. No attempt was made to dry the carbon blacks, apart from conditioning in the FMC cell over night in a stream of dry heptane. It is envisaged that the latter process would remove any loosely bound water from the carbon black surfaces, but more strongly bound water was likely to be retained after conditioning and hence influence the adsorption behaviour. This seemingly relaxed approach to sample drying was taken in order to produce results that may be representative of adsorption

TABLE I Commercial antioxidants investigated

Trade name (Supplier in parentheses)	Chemical structure	Molar mass
Irganox 1010 (Ciba)	Tetrakis [methylene (3,5-di-tert-butyl-4-hydroxyhydrocinnamate)] methane	1178
Irganox 1076 (Ciba)	octadecyl 3,5-di-tert-butyl-4-hydroxyhydrocinnamate	531
Irganox 1330 (Ciba)	1,3,5- Tris (3,5-di-tert-butyl-4-hydroxybenzyl)-1,3,5-triazine-2,4,6 (1H, 3H, 5H) trione	775
Irganox 3114 (Ciba)	1,3,5- Tris (3,5-di-tert-butyl-4-hydroxybenzyl)-1,3,5-triazine-2,4,6 (1H, 3H, 5H) trione	784
Cyanox 1790 (Cytec)	1,3,5- Tris (4-tert-butyl-3-hydroxy-2,6-dimethylbenzyl)-1,3,5-triazine-2,4,6 (1H, 3H, 5H)-trione	700

TABLE II Properties of carbon blacks studied

CB Type	Surface area		Particle size ^d nm.	Iodine Number (mg g ⁻¹)	DBPA Pellets cm ³ /100 g	Volatile Content ^d % w/w	pH ^c	Water content ^c % w/w
	STSA ^a (m ² g ⁻¹)	N ₂ multipoint ^b (m ² g ⁻¹)						
CB-A	86.8	107.1	22	119.6	96.6	1.5	8.5	1.01
CB-B	79.3	81.1	25	79.2	101.6	1	8.5	1.08
CB-C	85.1	113.2	25	78.2	72.5	3.5 ± 1	2.5	2.56
CB-D	370.5	542.8	13	173.3	91.3	8.5 – 12	2.5	8.59

^aStandard thickness surface area.

^bObtained by N₂ BET measurements.

^cObtained by Karl Fisher measurements.

^dObtained from (Cabot North American Technical report)²⁰.

processes occurring within a polyolefin matrix composite. It would obviously be impossible to maintain the absolute dryness of carbon black used in the commercial production of carbon black pigmented polyethylene (PE).

All others solvent/reagents, (*n*-Heptane and Chloroform) were of HPLC grade or 99% + purity where appropriate.

2.2. X-ray photoelectron spectroscopy (XPS)

The carbon black XPS spectra were obtained with a SSI-X probe (SS-100/206) spectrometer from Fisons (Surface Science Laboratories, Mountain View, CA), equipped with an aluminium anode (10 kV, 17 mA) and a quartz monochromator. The direction of photoelectron collection made angles of 55° and 73° with the normal to the sample and the incident X-ray beam, respectively. The electron flood gun was set at 6 eV. The vacuum in the analysis chamber was 2.5 × 10⁻⁷ Pa. The binding energies of the peaks were determined by setting the C (1s) component due to carbon only bound to carbon and hydrogen at a value of 284.2 eV. The peak areas were determined with a non-linear background subtraction. Intensity ratios were converted into atomic concentration ratios by using the SSI ESCA 8.3 D software package. The peaks were curve fitted using a non-linear least squares routine and assuming a Gaussian/Lorentzian (85/15) function.

2.3. FTIR, TGA and Karl-Fisher procedures

Samples isolated from the FMC were air dried and then diluted to 0.09% w/w with dried KBr (3 hours at

300°C), 0.2 g KBr discs were then pressed from these mixtures. KBr disks containing the pure carbon blacks were prepared in a similar manner. The samples were placed in a transmission cell fitted to a Nicolet 510 FTIR spectrophotometer (DTGS detector) with dry, CO₂ free air purge. Spectra were made up of 500 scans with a resolution of 2 cm⁻¹. Thermogravimetric analysis (TGA) was performed in a nitrogen atmosphere using a Netzsch TG 209 in a nitrogen atmosphere, samples (6–12 mg) were heated from 25°C to 900°C at 1°C min⁻¹.

In order to determine the water content of the pure carbon blacks studied, Karl Fisher tests were performed with a Kyoto MKC210 titrator coupled to an ADP-351 evaporator at 200°C in 20 min.

2.4. Flow micro-calorimetry

The FMC used was a Microscal 3V that has been upgraded to the all PTFE fluid path “I” (inert) specification. The Instrument was linked to the Microscal thermistor bridge-control unit whose output was fed to a Perkin-Elmer 900 series interface. The cell outlet was connected to a Waters 410 differential refractometer whose data was fed into the second channel of the 900 series interface. Energy calibration of the FMC was achieved via passage of a known quantity of electric power for a fixed time period through a filament integrated into the cell outlet connector. Calibration of the differential refractometer was achieved using a 20 μl calibrated loop. The 900 series interfaces were linked to a PC for data manipulation using Nelson Chromatography software, V.4.2.

For most of the additives, the carrier fluid was *n*-Heptane (Aldrich HPLC grade) stored over freshly

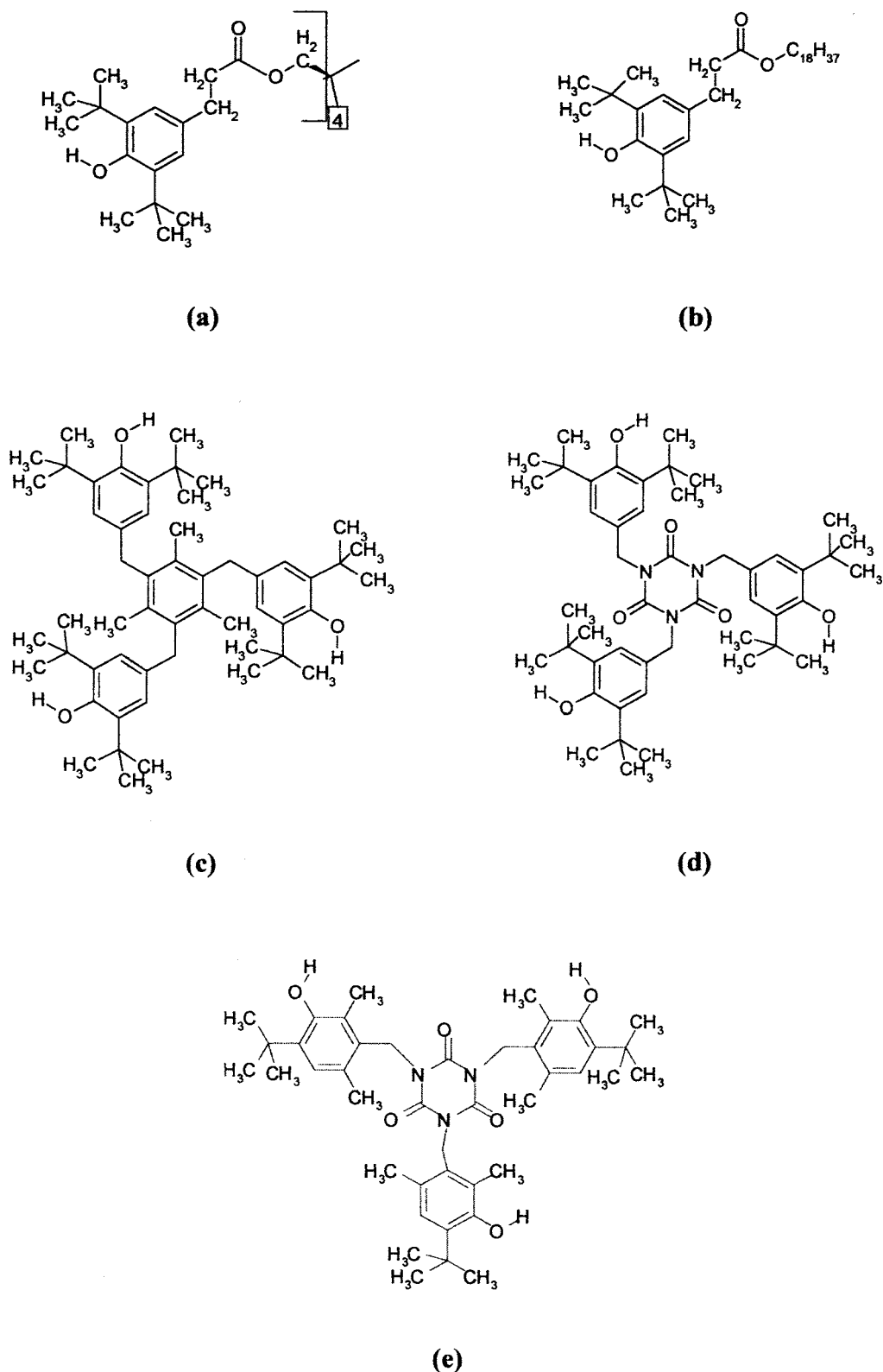


Figure 1 Structures of phenolic antioxidants investigated; (a) Irganox 1010, (b) Irganox 1076, (c) Irganox 1330, (d) Irganox 3114 and (e) Cyanox 1790.

activated (350°C, 3 hours) 4A molecular sieve. Decahydronaphthalene was used as the non-adsorbing probe.

The FMC studies were conducted using a cell temperature of 27°C ($\pm 1^\circ\text{C}$) and a probe concentration of 0.03% w/v. The solvent flow rate was 3.30 cm³ hr⁻¹ and sample size was 67.5 mg (± 0.5 mg). The cell temperature of the differential refractometer was 40°C and sensitivity was set to 4.

Carbon black powder aggregates between 60 and 80 mesh remained sufficiently aggregated during the FMC experiment not to pass through the sintered PTFE pad that forms the outlet filter of the Microscal L4P calibration outlet. After sieving to the indicated size range, the carbon black aggregates were weighed into a graduated tube such that the volume of aggregates was 0.15 cm³. The tube was gently tapped on the bench during filling to optimise the aggregate packing density.

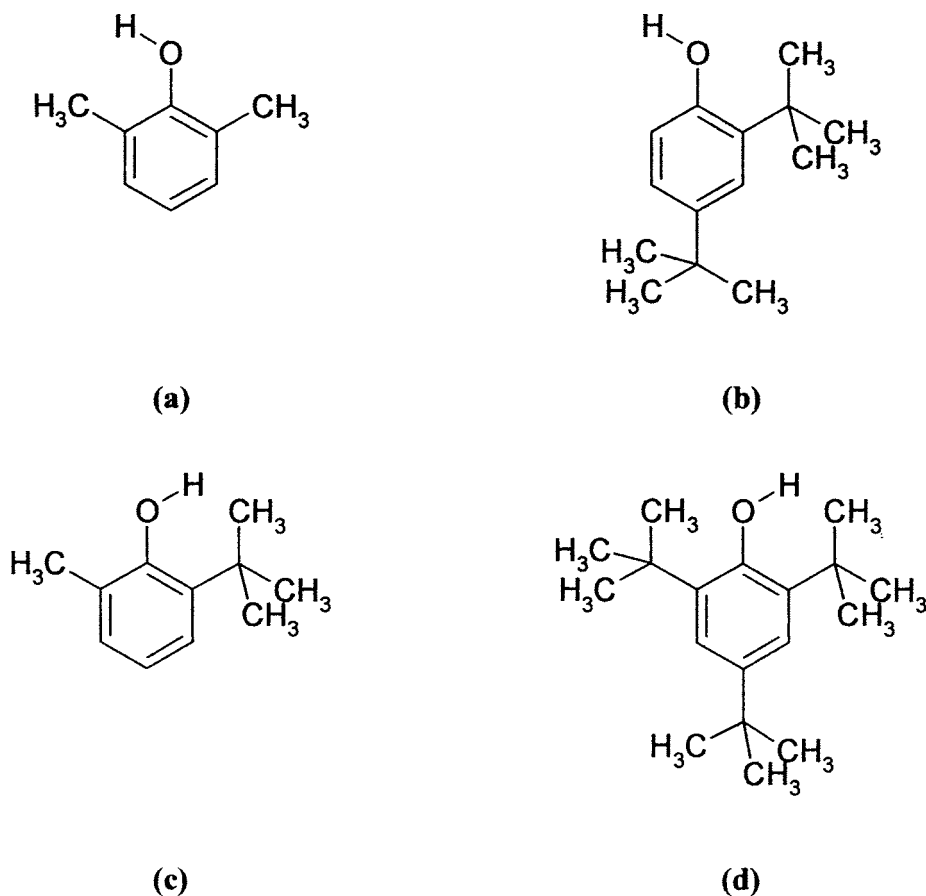


Figure 2 Structures of alkyl phenolic model compounds for investigation of steric hinderance of the phenolic OH; (a) 2,6 dimethyl phenol, (b) 2,4 di-*tert*-butyl phenol, (c) 2-*tert*-butyl 6 methyl phenol and (d) tri-*tert*-butyl phenol.

The measured charge was then introduced to the FMC cell by means of the purpose designed funnel. Negligible (<0.0001 g) amounts of carbon black remained in the graduated tube or on the walls of the cell charging funnel.

Samples were left to equilibrate at a carrier fluid flow rate of $0.033 \text{ cm}^3 \text{ hr}^{-1}$ over night at 27°C ($\pm 1^\circ\text{C}$). The flow rate was then increased to $3.3 \text{ cm}^3 \text{ h}^{-1}$ and the system left to settle for ca. 1 hr. Data collection was started, and after 5–10 minutes the inlet was switched from carrier fluid to the solution of the probe in the carrier fluid. After the refractive index data reached a stable limiting value (typically 80 to 110 minutes) the inlet was switched back to carrier fluid and the desorption processes recorded.

Thermal calibration constants were determined from an average of 2–3 peaks. The differential refractometer is then calibrated using the $20 \mu\text{l}$ loop, 7–8 calibration peaks were obtained. Non-adsorbing probe data was obtained once for each carbon type.

The amount of probe adsorbed was determined by normalisation of the non-adsorbing probe trace deflection to that of the adsorbing probe, once limiting deflection had been obtained. The deflection of the adsorbing probe is not altered. The non-adsorbing probe data was then offset in the signal domain by adding or subtracting a constant to the data so that its initial value was identical to that of the adsorbing data. The adsorbing data is then subtracted from the non-adsorbing data and the result saved as a separate file. The area of the re-

sultant peak was proportional to the amount of probe adsorbed. The constant of proportionality is the ratio of the mass of probe in the calibration loop, to the average area of the concentration calibration peaks. Using an identical approach, the amount of probe desorbed can also be calculated. Small but pronounced spikes in the thermal data were obtained when switching the inlet feed and these were used as time markers. For a more comprehensive review of the FMC technique, the reader is referred to Rothon's book [17].

In previous work carried out by the authors [18, 19] we have shown that the error of FMC measurements onto carbon black and magnesium hydroxide is usually $\pm 5\%$.

3. Results and discussion

3.1. Characterisation of the carbon blacks

Chemical analysis of the carbon black surfaces was carried out using X-ray photoelectron spectroscopy (XPS), FTIR, N_2 BET adsorption studies, Iodine adsorption and Karl Fisher measurements. Additional data were obtained from a Cabot North American Technical report [20]. The water content, volatile content and pH can be related to the hydrophilic character of the carbon black particle. For example, CB-D and CB-C have been oxidised with nitric acid and therefore have a higher surface concentration of oxygen containing functional groups than CB-B and CB-A. The FTIR and XPS analysis, which follows, effectively confirms the latter.

Differences between STSA and multi-point N₂ BET specific surface area values can be related to the porosity of the carbon blacks. Data shown in Table II, together with literature data [21, 22], indicates that CB-D is likely to have a porous surface. Micro-pores (<2 nm), meso-pores and macro-pores are present in this sample and are likely to affect its adsorption behaviour.

3.1.1. FTIR studies on pure carbon blacks

The FTIR results show that only CB-C and CB-D have a well-defined presence of functional groups on the surface, both have peaks that correspond to structures featuring carbonyl and carboxyl groups, however, CB-D shows a higher proportion of these groups. In general, these spectra are similar to examples found in the literature [23, 24]. The breadth of the carbonyl absorption band envelope (1735–1700 cm⁻¹) reflects a mixture of different groups attached to a polyaromatic structure (anhydrides, lactones (1735 cm⁻¹), aldehydes (1700 cm⁻¹). Due to the acidic nature of these two carbon blacks, some of these groups may be carboxylic acids (1700–1720 cm⁻¹). The XPS contribution at 531.5 eV corresponds to C=O (aldehydes, ketones and carboxylic acids) (Fig. 3). These infrared absorption bands are still present in spectra of heptane washed samples recovered from the FMC cell, therefore these functional groups are likely to be chemically attached to the carbon black surface and not associated with physically adsorbed molecules. The deconvoluted XPS data is in agreement with, and thus complements the FTIR data.

Other structures such as phenols, ketones, quinones, hydroquinones and anhydrides, may lay hidden within the broad absorption envelope of the C=C stretching vibrations of the polyaromatic structures of carbon black. However, such groups are detected by XPS at 534.5 eV which represent C-O linked to sp² carbons (such as Ph-O or O=C-O). Moreover, as observed in the literature, the intensity of the band at 1600 cm⁻¹ increases as volatiles content increases, therefore, the infrared absorption described above includes some oxygen functionality.

CB-B and CB-A do not show a carboxylic acid group (1700–1720 cm⁻¹). The presence of phenolic (C-O stretch at 1224 cm⁻¹) and carbonylic compounds in both blacks can be located between 1150 cm⁻¹ and 1300 cm⁻¹ [24].

From FTIR data, extrapolated values, from semi-quantitative analysis described by O'Reilly *et al.* [24], of COO- and C=O groups can be calculated. These values are close to calculated values obtained by titration of the studied blacks and are as follows; CB-D (about 0.2–0.25 meq · g⁻¹ of COOH and 1.8 meq · g⁻¹ of C=O groups); CB-C (≤0.1 meq · g⁻¹ of COOH and 0.5–0.75 meq · g⁻¹ of C=O groups); CB-B (≤0.7 meq · g⁻¹ of C=O groups) and CB-A (about 0.61 meq · g⁻¹ of C=O groups). No carboxylic acid groups were detectable on the latter two carbon blacks.

It is also evident that the presence of water in the carbon black and KBr gives rise to a broad OH stretching band, which obscures OH absorptions associated with phenolics and carboxylic acids. However, O'Reilly [24]

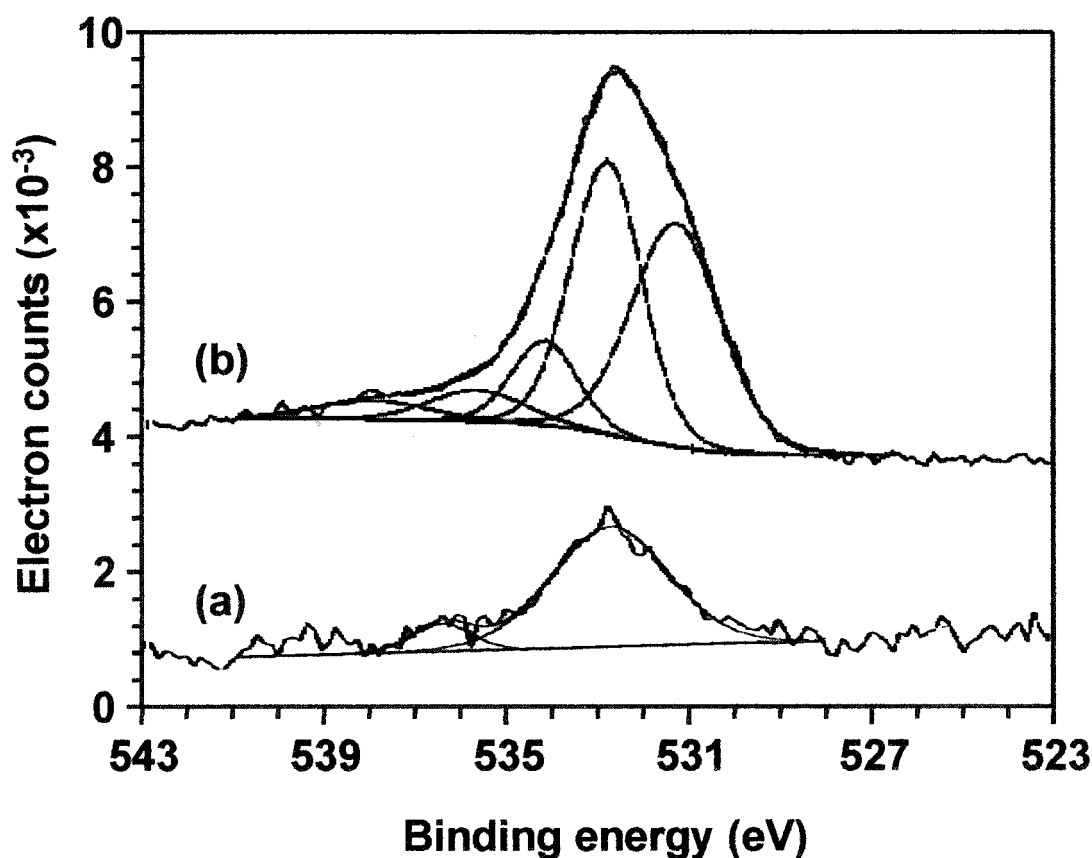


Figure 3 High resolution O(1s) spectra showing curve fitting and deconvolution for; (a) CB-A and (b) CB-D.

TABLE III Detailed functional composition (ratio O/C, S/C) of the different carbon blacks

Sample	O=C O-S Carboxylic Aldehyde, Ketone,	O-C Hydroxyl, Ethers	O-C Phenol Anhydride	H ₂ O O ₂	S-C	SO ₂ Sulphones	SO ₄ Sulphates	C-N	NO ₂
Binding energy (eV)	531.5	533.1	534.5	535.8	163.8	166.4	168.8	400	405
CB-A	0	0.0049	0	0.0006	0.0002	0	0	0	0
CB-B	0	0.0082	0	0.0006	0.0043	0.0006	0.0003	0	0
CB-C	0.0163	0.0127	0.0046	0.0024	0.0023	0.0005	0.0006	0.0027	0.0014
CB-D	0.0245	0.0238	0.0068	0.0037	0.0008	0	0.0016	0.0019	0

has shown that no discernible phenolic OH bands were apparent at 3600 cm⁻¹, even after subtraction of the OH absorption band from adsorbed H₂O.

3.1.2. Analysis of carbon black surface chemistry by X-ray photoelectron spectroscopy (XPS)

From the global spectra, corresponding to the collection of electrons with binding energies between 0 and 1100 eV, the surface elemental composition of each carbon black was estimated. In addition to carbon, the presence of oxygen and sulphur on each CB surface was detected. Nitrogen was also detected on CB-C and CB-D (Table III).

From the O/C ratio, a direct indication of the extent of oxidation of the CB surfaces is obtained, and can be ranked as follows; CB-D > CB-C > CB-B > CB-A. There is a ten-fold difference between the lowest and highest surface oxygen concentration.

CB-A appears to be the “cleanest” black, as no nitrogen and only a very small quantity of sulphur can be detected. The level of oxidation of CB-A is very low and is reflected in the lowest surface oxygen concentration of all the samples examined. CB-B contains the highest sulphur level and has a surface oxygen concentration almost twice that of CB-A. The two highly oxidised samples, CB-D and CB-C, predictably, have the highest surface oxygen concentration. Some sulphur and nitrogen containing functional groups could also be detected on the surfaces of the latter two samples. Whatever the sample analysed, we can emphasise that oxygen based functional groups always represent the major contribution to the surface chemistry of these carbon blacks.

In order to identify and even quantify the different functional groups associated to O, N and S, high-resolution spectra of C (1s), O (1s), N (1s) and S (2p) photoelectrons were produced. These spectra have been deconvoluted so the contributions of the various functional groups, to the overall peak envelope, can be estimated. The latter approach is described in the literature by Papirer and Lacroix [25].

Due to the polyaromatic nature of the carbon black, curve fitting of the C (1s) spectrum is difficult. The main C (1s) component at 284.2 eV, corresponding to non-functionalised carbon (i.e., C-C, C-H), shows unusual asymmetry which was impossible to model with the processing program used. This asymmetry also affected

the components at higher binding energies (carbons linked to heteroatoms). If curve fitting is performed regardless of this asymmetry, over-estimation of contributions, arising mainly from oxidised carbons (i.e., O-C, O=C, O-C=O) occurs. Rather than trying to correct this analytical error by attempting to model this asymmetry (which would be a computationally intense process), a deeper interpretation and discussion based on the oxygen (O (1s)) peak was preferred.

Fig. 3 displays high-resolution spectra of oxygen (O1s) for CB-A and CB-D. Peak areas are directly proportional to the atom fraction. In addition to the simple increase of extent of oxidation from CB-A to CB-D, deduced earlier from O/C ratios, the O (1s) spectra indicate qualitative variations in the nature of the oxygen content. For CB-C and CB-D, the O (1s) peak exhibits an important shoulder at lower binding energies resulting from the presence of functional groups produced under strongly oxidising conditions. In order to proceed further in this qualitative interpretation, deconvolution curve fitting of these high-resolution spectra, using the previously described parameters, has been performed. The curve fit and deconvolution are also shown in Fig. 3.

CB-A gave a simple curve with two components near 533 eV and 536 eV respectively. The former corresponds to C-O functional groups (mainly ethers/hydroxyls linked to sp³ hybridised carbon) and the latter results from adsorbed species (H₂O and O₂). The O (1s) peak of CB-B is deconvoluted into the same contributions at 533 and 536 eV. However, a third component, associated with satellite (π - π^*) shake-up, appears at 537.6 eV, and thus explains the more pronounced shoulder appearing at higher binding energies. Interpretations of the CB-C and CB-D curves were more complex but similar features to CB-A and CB-B remained apparent. However, with CB-C and CB-D, two additional components at 531.5 eV and 534.5 eV were present. Oxygen at 534.5 eV represents C-O linked to sp² hybridised carbons (such as Ph-O or O=C-O). The contribution at 531.5 eV corresponds to oxygen with a high density of bonding electrons; they can be associated to C=O (aldehydes, ketones, carboxylic acids) or S-O (sulfones, sulphates). Therefore a higher level of oxidation of carbon black does not only imply a higher oxygen content, but also a surface featuring different chemical composition with more acidic functional groups.

The different sp² spectra are grouped in Fig. 4. Again, from their high-resolution spectra, we observed

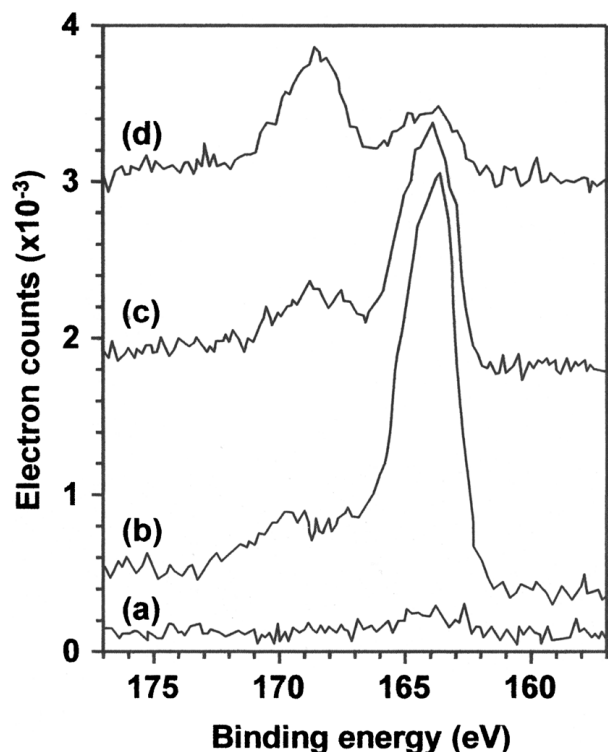


Figure 4 sp^2 spectra of showing the relative level and nature of sulphur based species for; (a) CB-A, (b) CB-B, (c) CB-C and (d) CB-D.

significant differences in the sulphur contents of the carbon blacks. As with the O (1s) data, curve fitting and deconvolution was performed in order to gain further insight into the chemical nature of the sulphur containing functional groups. The CB-A curve indicates a very small component at 163.8 eV, corresponding to $S-C$. This component is also present on the other three samples and the relative levels of $S-C$ based species can be ranked as follows: $CB-B > CB-C > CB-D$. On these latter carbon blacks, two other sulphur containing moieties were detected. The first appears at 166.4 eV and corresponds to sulphones and the second appears at 168.8 eV and is due to sulphates. The level of SO_4 can be ranked as follows: $CB-D > CB-C > CB-B$, this trend is exactly opposite to that for $S-C$.

Finally, an estimate was made of the relative amount of each chemical species identified respectively in the fitting studies, by combining them with the quantitative elemental composition described earlier in Table I. In other words, the global O and S content can be split into their different components. The detailed results are reported in Table III.

Given the considerations reported by Papirer [25] concerning the relative particle size (d) and the depth of escape of the photoelectrons (x) by which $x \cong d = 15-20$ nm; we can assume that the amounts of oxygen, sulphur and nitrogen estimated would coincide with the estimations of compositions made by chemical analysis. According to our FTIR results, oxygen containing groups were detected on the surface of the carbon blacks, and it can be concluded that these functional groups are located on the CB surface, as reported in the literature [5]. The sulphur levels obtained from XPS are different to those reported in the latter paper, where the presence of sulphur is distributed within the bulk

of the carbon black. However, if the sulphur is equally spread in all the blacks, the results for different samples of CB will be valid in order to compare the relative sulphur content.

3.2. Adsorption of primary antioxidants onto the carbon black samples

Different stabilisers and carbon blacks were chosen according their chemical nature and surface features. CB-A and CB-B, both used in plastic applications, are studied with all the stabilisers chosen while for CB-C and CB-D their interaction with Irganox 1010 and Cyanox 1790 was examined in order to compare the different activity of the four blacks with commercial stabilisers.

3.2.1. Overall adsorption activity

Adsorption and desorption energies resulting from the interactions of the different primary antioxidants with the carbon blacks were determined by FMC. A difference in the degree of phenolic hydroxyl obstruction by alkyl groups was found to be the main factor affecting the adsorption activity. With all the carbon black samples investigated Cyanox 1790 (with *tert*-butyl and methyl groups in the 2 and 6 positions, relative to the phenolic OH) showed the strongest adsorption activity. In contrast Irganox 1010 (with *tert*-butyl groups in the 2 and 6 positions relative to the phenolic OH) shows substantially weaker adsorption activity and in some cases is close to the limit of detection (Fig. 5).

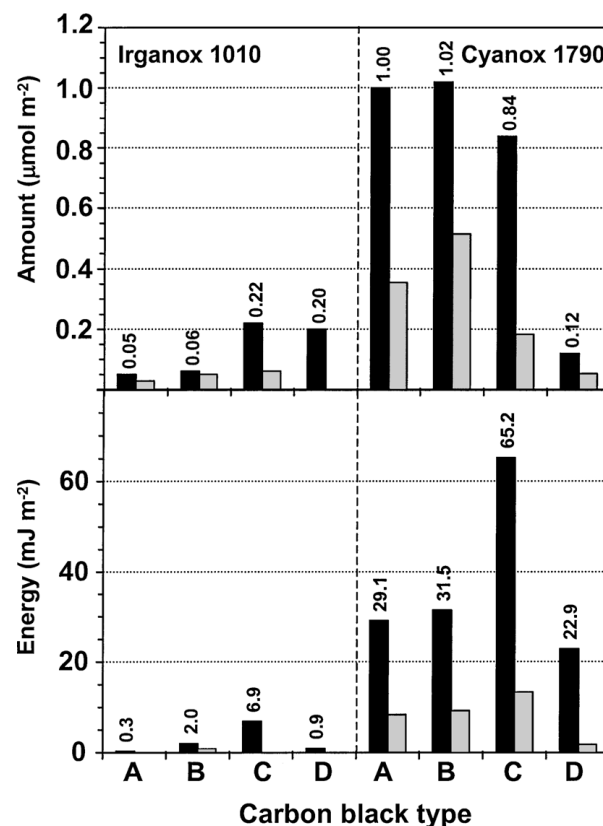


Figure 5 FMC data for adsorption of Irganox 1010 and Cyanox 1790 on to the four carbon blacks from heptane (the sign of adsorption energy change has been reversed to aid comparison); ■ adsorption; ▒ desorption.

Even lower adsorption activity was observed with Irganox 1330 (no adsorption on CB-A and CB-B) and Irganox 3114 (ca. 0.2 mJ m^{-2} on CB-A and CB-B) as they share the same 2, 6 di-*tert*-butyl phenolic functionality as Irganox 1010, but lack the ester functionality. The contribution of the ester grouping is further highlighted by adsorption of Irganox 1076 (1.9 mJ m^{-2} and 1.3 mJ m^{-2} on CB A and CB-B, respectively). The relatively high values of heat of adsorption of the latter reflect greater steric accessibility of the ester group. These results agree with the literature [4], where adsorption activity was found to be influenced by molecular shape; rod-shaped molecules such as Irganox 1076 will show a higher adsorption activity than those that are square shaped as for Irganox 1010.

It is surprising that the 1, 3, 5-triazine-2, 4, 6 (1H, 3H, 5H)-trione core of Irganox 3114 does not contribute in any significant way to its adsorption activity. FTIR studies, however, on samples recovered from the FMC cell after treatment with Cyanox 1790, that shares the same core structure, do indicate interaction of the 1, 3, 5-triazine-2, 4, 6 (1H, 3H, 5H)-trione core with the carbon black surface. With the latter stabiliser the core is somewhat less hindered and molecular modelling studies indicate that interaction with a surface will be possible.

The adsorption activity of a given stabiliser is also of course influenced by the surface chemistry of the carbon black just as much as the chemical nature of the stabiliser itself. Therefore comparison of the adsorption behaviour of a given stabiliser onto the different carbon black samples can afford some insight into the surface chemistry of the carbon blacks. The adsorption energies for Cyanox 1790 and Irganox 1010 with the four carbon blacks can be ranked as follows:

Cyanox 1790

CB-C > CB-B > CB-A > CB-D.
 $(65.2 \text{ mJ m}^{-2}) > (31.5 \text{ mJ m}^{-2}) > (29.1 \text{ mJ m}^{-2}) > (22.9 \text{ mJ m}^{-2})$

Irganox 1010

CB-C > CB-B > CB-D > CB-A.
 $(6.9 \text{ mJ m}^{-2}) > (2.0 \text{ mJ m}^{-2}) > (0.9 \text{ mJ m}^{-2}) > (0.3 \text{ mJ m}^{-2})$.

It is evident that CB-C exhibits the greatest overall adsorption activity. This is because it has more active adsorption sites per unit surface area than CB-B and CB-A, and is reflected in its surface elemental composition (Table III). The relatively high volatile content (3.5%) of CB-C also reflects a high level of oxidised functional groups [5]. FTIR spectra revealed the presence of functional groups associated with carbonyl and carboxyl species. The high water content (2.56%), part of which may remain on the surface even after conditioning in the FMC overnight with dry heptane, is another factor affecting the adsorption behaviour of CB-C.

Although CB-D has the higher volatile content (8.5–12%), together with strong acidity, when dispersed in water (pH of 3 ± 1), it shows the lowest adsorption activity with Cyanox 1790. FTIR and XPS analysis confirms the presence of acidic functional

groups associated to carbonyl and carboxyl species. The XPS analysis clearly indicates that CB-D is the most highly oxidised sample, however, the surface area normalised FMC data is not consistent with this finding. This could be explained by the existence of a “hydrogel effect”. Such a “hydrogel effect” appears when there is a high concentration of polar groups on a surface; they interact with water molecules that form a gel-like structure (3D network by hydrogen bonding), which effectively blocks surface adsorption sites. [26, 27].

In addition, interactions between closely adjacent functional groups on the CB surface could result in the loss of adsorption activity; particularly when the interactions between these surface groups are stronger than the interactions between the surface groups and the adsorbate molecule. Thus the functionalities, which are believed to be on the edges of the CB basal planes, would interact with themselves resulting in significantly reduced interactions with adsorbate molecules. In such a situation, it is possible that the surface activity of a CB will reach a maximum at a certain concentration of functional groups. Once this limit is exceeded, mutual interaction dominates and adsorption activity decreases. Of course, the activity would also depend on the nature of these functionalities. Porosity is also a factor to be taken into account and will affect the adsorption of additives, particularly phenolic compounds, as described in the literature [28].

Carbon black CB-B exhibits the second greater overall adsorption activity for Irganox 1010 and Cyanox 1790 with respect to the other carbon blacks studied. Again, CB-B shows features that explain its behaviour. As CB-B has a lower surface oxygen concentration (0.0097 O/C) and volatile content (1%) than CB-C (3.5%), but similar surface area ($79.3 \text{ m}^2 \text{ g}^{-1}$), it can be deduced that the latter has a lower concentration of functional groups per unit surface area than CB-C. There are also differences, however, in the nature of the functional groups present on each carbon black surface and their population distribution. CB-C has oxidised functional groups like SO_4 and $\text{C}=\text{O}$ (carbonyls and carboxyls) whilst CB-B has mainly O-C and S-C. The main functional groups on CB-B are O-C and S-C (alcohols, thiols, etc, by XPS analysis). The concentrations of sulphates and sulphones are very low (10 times lower than the former ones), hence their contributions are probably negligible. Therefore, the difference between CB-A and CB-B can be justified by the difference in O-C and S-C concentration. This is consistent with the type and relative impurity of the oil feedstock used to produce CB-B, which has a higher sulphur content and oxidised hydrocarbon content than that used to produce CB-A.

Because of the “hydrogel effect” and the mutual interactions between surface functional groups, CB-D shows a reduced level of interaction with phenolic compounds, relative to the other carbon blacks investigated. However, CB-D appears to be somewhat more active than CB-A, with Irganox 1010, probably due to a higher selectivity of CB-D towards the ester group present in this antioxidant, and because of its more acidic character. Again, the relatively large amount of

water on CB-D (8.59%) can explain the very low activity of its surface, despite the high surface concentration of oxygen containing functional groups. A significant proportion of this water probably remained on the surface of CB-D even though the sample in the FMC cell was flushed overnight with dry heptane.

It can be concluded, from the discussion above, that there are two main factors affecting the adsorption of phenolic compounds onto carbon black. The first is the influence of steric hindrance of the phenolic hydroxyl groups caused by alkyl groups in the ortho positions. The second factor is the carbon black surface chemistry.

3.2.2. Level of antioxidant adsorption

In general, the observed quantities (Fig. 5) can be related to the values of adsorption/desorption energy described previously and to the molar mass of the probes. Thus, probes with a high molar mass and high activity show the greatest values of amounts adsorbed. As was expected for all the carbon blacks Cyanox 1790 shows the highest level of adsorption (up to $1.02 \mu\text{mol m}^{-2}$, i.e., 3–6% w/w of carbon black) whilst the other primary antioxidants show far lower activity with only small differences between the types investigated. Irganox 3114 and Irganox 1330 show some adsorption ($0.03\text{--}0.10 \mu\text{mol m}^{-2}$, i.e., 0.6% w/w of carbon black).

In the majority of cases most of the adsorbed material is readily desorbed and only a small fraction remains on the surface, except in the case of Cyanox 1790 where the amounts remaining are around 2–4% w/w with all the carbon blacks. Irganox 1010 is also strongly retained on CB-C (Fig. 5). At this stage in the discussion the possibility of adsorption of the antioxidants as aggregates of molecules (perhaps in a micelle-like arrangement) must be considered, as such effects have been described in the literature [4]. Because of the non-polarity of the *n*-heptane carrier fluid and the high polarity of the antioxidants, one can expect that intermolecular attractions will cause aggregation of antioxidant molecules.

Thus, we found in some cases that the levels of antioxidant adsorption were greater than the theoretical monolayer level, calculated from the molecular area of the adsorbate and the specific surface area of the carbon black. For instance, Cyanox 1790 could undergo multilayer adsorption, typically the degree of coverage was 1.7–2.2 equivalent monolayers. However, because of the possible aggregation of the additives, and the selective adsorption on specific sites of the carbon black surface, adsorption of such aggregates on specific adsorption sites could take place. As a result of this effect, some parts of the carbon black may still remain uncovered despite the apparent multilayer adsorption.

Other antioxidants such as Irganox 1010, Irganox 1076 Irganox 1330, Irganox 3114, Irganox 1330 and the model compound phenol, tended to adsorb to 0.2–0.7 monolayers. With CB-C, Phenol and Irganox 1010 practically cover the whole surface of the carbon black. However, the possibility of inhomogeneous adsorption on the carbon black surface must also be

considered and would result from aggregation of the additive molecules at selected sites on the surface. Considering the very heterogeneous surface of carbon black (with large planes of aromatic carbons and rows of functional groups at the edges and intersections of planes), non-uniform adsorption would indeed be expected. In order to understand the manner in which adsorption takes place, further work would be needed using techniques with different penetration depths, such as XPS at different angles of analysis, SIMS, and Atomic Force Microscopy (AFM).

With each antioxidant, the four carbon blacks show varying levels of adsorption. In general, for a given additive, the molar amount of antioxidant adsorbed per unit area must be taken into account. The latter parameter is influenced by two factors that are; the surface concentration of functional groups which have an affinity for the functional groups of the additives, and the chemical nature of these surface functional groups. The specific surface area also plays an obvious role, as a carbon black with a higher specific surface area but having the same concentration of functional groups, will adsorb a greater amount of additive per unit mass than an equivalent carbon black with lower surface area. The molar amount of Cyanox 1790 adsorbed per unit surface area of carbon black shows a different ranking to the adsorption energy from heptane:

$$\text{CB-B} \geq \text{CB-A} > \text{CB-C} > \text{CB-D}$$

(Molar amount adsorbed).

$$\text{CB-C} > \text{CB-B} > \text{CB-A} > \text{CB-D}$$

(Adsorption energy).

On this basis, CB-C (which has the highest adsorption activity with Cyanox 1790) has a low concentration of very active (energetic) adsorption sites, such as carboxylic acid, sulphate and sulphone groups, and phenolic hydroxyl groups etc, as indicated in the FTIR and XPS data. Therefore the energy of interaction per molecule of Cyanox 1790 is greatest on CB-C. The relatively high levels of adsorption per unit surface area observed with CB-A and CB-B may be explained by structural and topological differences. Thus, CB-A contains a lower concentration of functional groups and consequently would have a smoother surface, which would result in an increase in the contribution of the dispersive interactions associated with the semi-graphitic basal planes of carbon black. Such interaction would result in weaker overall adsorption energy may lead to greater number of molecules adsorbed per unit area.

On the other hand, CB-B has a higher surface concentration of polar active sites, than CB-A, but is deficient in this respect relative to CB-C. CB-B may retain some CB-A surface features such as the greater ability to form dispersive interactions, via the semi-graphitic basal planes, than CB-C. This results in a greater overall concentration of active sites on CB-B than on CB-A.

Considering the surface analyses carried out and relevant literature [22], CB-D is a highly oxidised carbon black featuring a micro-porous surface (pore size < 2 nm). However, the previously described

“hydrogel effect” and/or mutual interactions between adjacent functional groups, probably results in deactivation of the majority of polar active sites, attractive to Cyanox 1790. The latter effects cause CB-D to adsorb less Cyanox 1790 than CB-C and CB-B, despite the very high concentration of polar surface groups on CB-D.

Irganox 1010 shows a different situation. The amount adsorbed (per unit area) for Irganox 1010 can be ranked as follows:

CB-C > CB-B > CB-A > CB-D

(Molar amount adsorbed per unit surface area)

CB-C > CB-B > CB-D > CB-A

(Adsorption energy)

It is remarkable that the distribution of active sites that strongly adsorb Irganox 1010 differ somehow from those which adsorb Cyanox 1790. CB-C again appears to bear the greater number of strongly active adsorption sites, together with a high overall concentration of these sites. Similar behaviour is shown by CB-B, but to a lesser extent. CB-D has some very active sites but these will be largely deactivated due to the reasons given earlier, associated with the “hydrogel effect” and mutual group interaction. CB-A is again shown to have the lowest concentration of highly polar active species (as confirmed by XPS). However, the level of adsorption of Irganox 1010 and Cyanox 1790 on CB-A is greater than that on CB-D due to the dispersive contribution from the semi-graphitic basal planes.

The interaction between carbon black and Irganox 1010 would be expected to be via hydrogen bonding with the phenolic OH. However, the phenolic OH group of Irganox 1010 has low activity because it is sterically hindered (shielded) by the tertiary butyl groups ortho to the OH. The effect of such steric hindrance is investigated in the next section. The only functional group on Irganox 1010 able to strongly interact is therefore the ester group. This can interact with acidic sites like carboxylic acid groups (detected on CB-C and CB-D), and phenolic groups on the carbon black surface. In addition, dispersive forces can contribute in the CB-stabiliser interactions.

The interaction between Cyanox 1790 and carbon black will have a stronger phenolic OH hydrogen bonding contribution than Irganox 1010 due to reduced shielding of the phenolic OH (Fig. 1). In this case, strong interaction between the phenolic hydroxyl group of Cyanox 1790 and carbon black surface groups, such as carboxylic acids (detected on CB-C) and phenols, will occur. In addition, the phenolic hydroxyl of Cyanox 1790 will have affinity towards Brønsted base sites, originating from impurity metal oxides present in low concentration, on the surface of the blacks.

3.3. Effect of steric hindrance on the adsorption of phenolic model compounds onto carbon black

In order to further investigate the effect of steric hindrance of the phenolic hydroxyl groups of the additives

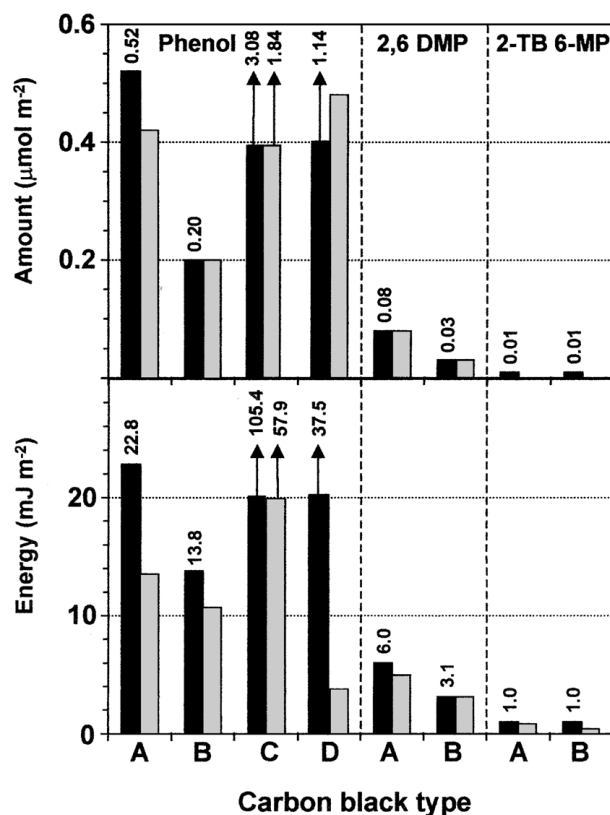


Figure 6 FMC data for adsorption of phenol on to the four carbon blacks and adsorption of 2,6 dimethyl phenol and 2-*tert* butyl 6-methyl phenol onto CB-A and CB-B (all from heptane) (the sign of adsorption energy change has been reversed to aid comparison); ■ adsorption; □ desorption.

on their adsorption behaviour; a range of model compounds, with varying degrees of phenolic OH steric hindrance was studied.

3.3.1. Overall adsorption activity

Data presented in Fig. 6 shows that increasing steric hindrance of the phenolic hydroxyl groups decreases the overall adsorption/desorption activity of the model compounds onto CB-A and CB-B. 2,4 di-*tert*-butyl phenol and 2,4,6 tri-*tert*-butyl phenol were also investigated but the data is not shown in Fig. 6. The latter probe showed no adsorption as the phenolic OH was completely shielded by the *tert*-butyl groups. However, 2,4 di-*tert*-butyl phenol gave an adsorption energy between that of 2,6 dimethyl phenol and 2-*tert* butyl 6-methyl phenol. Such a trend is not unexpected as an additional *tert*-butyl group in the para position will cause less steric hindrance of the phenolic OH than the methyl group of 2-*tert* butyl 6-methyl phenol.

Similar adsorption trends were observed with CB-A and CB-B with phenol and 2,6 dimethyl phenol (2,6 DMP). However, CB-A is shown to be more active than CB-B, due to the reduced concentration of acidic sites on the former carbon black, resulting in higher basicity and hence stronger interaction with phenol ($pK_a = 9.98$) and 2,6 dimethyl phenol. The stronger interaction of CB-A with phenol may also be due to dispersive interactions between the π -electron clouds of the smooth basal planes of CB-A and the π -electron clouds in the benzene ring of phenol.

In order to compare the four carbon black pigments, phenol was used as a model probe (Fig. 6). The adsorption energy of phenol can be ranked as follows:

$$\text{CB-C} > \text{CB-D} > \text{CB-A} > \text{CB-B}$$

The behaviour of CB-C is consistent with the above conclusions. Thus, this is the carbon black with the greatest effective concentration of highly active adsorption sites, despite the fact that CB-D has the greatest concentration of oxygen containing functional groups. This is due to the previously mentioned “hydrogel effect” and mutual interactions between adjacent surface functional groups of CB-D. Somewhat unexpectedly, phenol reacts more strongly with CB-D than with CB-A and CB-B. This may be due to the high acidity of phenol, relative to the stabilisers, and its small molecular size. Such high acidity may mean that phenol can compete with the mutual interactions between adjacent functional groups of CB-D. The porosity of CB-D could also play an important role in phenol adsorption, as this molecule may be small enough to be adsorbed within pores that are too large for stabiliser molecules to fit into. Such phenol adsorption mechanisms have been studied by Asakawa *et al.* [28] using inverse gas chromatography (IGC).

Finally, even though CB-B is a more oxidised carbon black than CB-A, it has a smaller quantity of surface groups that are attractive to phenol, relative to the other blacks examined. This observation provides insight in to how phenol is adsorbed on to carbon black. When the mechanism of phenol adsorption involves dispersive and polar interactions, as in the case of CB-A, the former can give the strongest contribution to the adsorption energy. Therefore the final sum of attractive force results in a higher adsorption energy with CB-A (22.8 mJ m^{-2}). In such a case, the phenol molecules are likely to adsorb horizontally on the CB surface [28]. Data in Table II (the difference between STSA point and multi-point BET surface area values) indicates that CB-A may have more porosity in its surface than CB-B. This increased porosity in the former may also contribute to the higher heat of interaction of phenol with this carbon black. With CB-A, the phenol molecules could also be adsorbed in the pores by dispersive interactions between the phenol aromatic ring and the walls of the pores [28]. The difference between the adsorption and desorption energies can be related to the irreversibility of the adsorption mechanism. CB-D shows a higher irreversibility (i.e., greater probe retention) than the other carbon blacks. This effect could be explained by a greater microporosity of this CB pigment. In cases where the relative acid-base strength of the absorbent and adsorbate is increased, one can expect increasing retention of the probe because of stronger bonding.

3.3.2. Level of model compound adsorption

Except for phenol, and 2,6 Dimethyl phenol, the amounts adsorbed for the rest of the model compounds

are too small to be properly resolved (Fig. 6). The level phenol adsorption can be ranked as follows:

$$\text{CB-C} > \text{CB-D} > \text{CB-A} > \text{CB-B} \\ (3.08) > (1.14) > (0.52) > (0.2) (\mu\text{mol m}^{-2})$$

As an identical ranking exists for adsorption energy, it may be inferred that the amount adsorbed corresponds to the adsorption energy. Therefore, CB-C shows the highest area concentration of highly active sites that result in it having the highest overall adsorption activity (Fig. 6).

CB-D shows that with phenol the “hydrogel effect”, and/or mutual interaction between surface groups can be overcome if probe interactions are of sufficient strength and possibly of a similar nature to the mutual interactions themselves. The fact that CB-A adsorbs more phenol can be explained by the explanations associated with micro-pores and a greater concentration of basic adsorption sites compared with CB-B. Some of these basic sites could be the basal graphene layers (Lewis base like) present on the carbon black surface [5, 29].

The same parallel behaviour is found with 2,6 dimethyl phenol; it is again evident that CB-A adsorbs more than CB-B.

3.4. FTIR studies on carbon black samples retrieved from FMC cell

Infrared absorptions assignable to Cyanox 1790 cannot be resolved on CB-A or CB-B even though the level of adsorption (per unit area) was relatively high. However, analysis of FMC treated CB-C and CB-D does show absorptions associated with Cyanox 1790, at 2960 cm^{-1} , 1464 cm^{-1} , 1430 cm^{-1} , 1408 cm^{-1} , 1213 cm^{-1} and 1174 cm^{-1} (Fig. 7). A shift in the carbonyl peak of Cyanox 1790 from 1702 cm^{-1} , in the

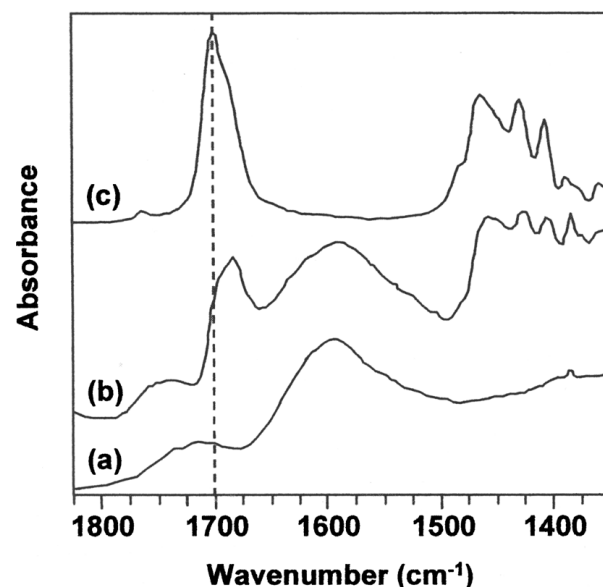


Figure 7 FTIR transmission spectra of: (a) pristine CB-D, (b) CB-D recovered from the FMC cell after adsorption of Cyanox 1790 and (c) Cyanox 1790.

unbound state, to 1685 cm^{-1} in the adsorbed state, shows that the adsorption is partly via the carbonyl groups of the 1,3,5 triazine-2,4,6 (1H, 2H, 3H) trione hub structure. These carbonyl groups could interact via hydrogen bonding with carbon black surface groups having labile hydrogen, such as phenols and carboxylic acids.

Irganox 1010 is adsorbed to such low levels on CB-A and CB-B that it cannot be detected by FTIR. However, some weak absorptions from Irganox 1010 are evident on CB-C and CB-D. No information regarding the mode of adsorption can be acquired from the spectral data obtained.

4. Conclusions and further work

New insight into factors affecting the adsorption of hindered phenolic stabilisers onto carbon black surfaces has been acquired using flow micro-calorimetry in conjunction with FTIR. The structural features of stabilisers that affect the strength and level of adsorption can be ranked as follows, in decreasing order of importance.

1. *Steric hindrance of phenolic OH groups*, many stabilisers have *tert*-butyl groups in the 2 and 6 positions relative to the OH group, in such cases the level of steric hindrance results in an inability to adsorb. Replacement of one of the *tert*-butyl groups with a methyl group significantly increases the accessibility of the phenolic OH to adsorption sites on carbon black surfaces and can lead to a 20-fold increase in the adsorption energy, resulting in strong retention of the stabiliser on the carbon black.

2. *Ester groups*, have been shown mildly contribute to adsorption activity, possibly via hydrogen bonding and dipole—dipole interactions with carbon black surface functional groups. The structure of the stabiliser must be such that the ester groups have access to the filler surface (e.g., Irganox 1076 rather than Irganox 1010, where the contribution from the ester groups is apparent but not very strong).

3. *1,3,5 triazine-2,4,6 (1H, 2H, 3H) trione core structures*, given sufficient steric access to surface adsorption sites, these species can interact with carbon black surfaces. Carbonyl shifts in FTIR data have shown that surface interactions occur with this type of core structure if the benzyl phenolic arms of the molecule are not hindered by *tert*-butyl groups in 2 and 6 positions, relative the phenolic OH. Replacement of one of these *tert*-butyl groups with a methyl group enables sufficient interaction of the 2,4,6 (1H, 2H, 3H) trione core structure with the carbon black surface to cause a perturbation of the trione carbonyl vibration frequency.

Carbon blacks with a range of oxygen contents were investigated and enabled factors affecting adsorption associated with the surface chemistry of the carbon black to be studied. The most significant aspect arising from this part of the study is that adsorption capacity does not necessarily monotonically increase as the surface concentration of functional groups increases. Rather, there is likely to be a critical surface concen-

tration of functional groups above which adsorption of water and mutual interactions between adjacent functional groups causes the adsorption capacity to fall dramatically. The importance of dispersive interactions together with adsorption in pores has also been highlighted by some of the data obtained in this study.

This study forms part of a larger programme in which adsorption behaviour of a comprehensive range of stabilisers is studied, including hindered amine light stabilisers and secondary antioxidants. In addition a detailed study has also been undertaken on the characterisation of the carbon black surfaces by monitoring the adsorption behaviour of simple acidic and basic molecules. These studies will be reported separately. The levels of adsorption achievable with some of the carbon black/stabiliser combinations may be sufficient to enable carbon black to act as a controlled release reservoir for stabilisers. This aspect will be examined in a future publication.

References

1. S. BANDYOPADHYAY and D. K. TRIPATY, *J. Appl. Sci.* **58** (1995) 719.
2. J. WOLFSCHWENGER, A. HAUER, M. G. GAHLEITNER and W. NEIBL, in Proceedings Eurofillers '97 (British Plastics Federation, Manchester, UK, 1997) p. 375.
3. C. M. LIAUW, A. CHILDS, N. S. ALLEN, M. EDGE, K. R. FRANKLIN and D. G. COLLOPY, *Polym. Degrad. Stab.* **65** (1999) 207.
4. A. P. D'SILVA, *Carbon* **36** (1998) 1317.
5. J. B. DONNET, R. C. BANSAL and M. J. WANG, "Carbon Black, Science and Technology" (Marcel Dekker Inc., New York, 1993).
6. M. H. POLLEY, W. D. SCHAEFFER and W. R. SMITH, *J. Am. Chem. Soc.* **73** (1951) 2161.
7. M. J. WANG, S. WOLFF and J. B. DONNET, *Rubb. Chem. Technol.* **64** (1991) 714.
8. A. I. MEDALIA, "Carbon Black" (Medalia Associates, Inc., Mass., USA, 1991).
9. J. A. MENÉNDEZ, *Thermochimica Acta* **312** (1998) 79.
10. A. J. GROZECK, *Proc. Roy. Soc. London* **A314** (1970) 473.
11. *Idem.*, *Carbon* **6** (1987) 717.
12. A. J. GROZECK and G. AHARONI, *Langmuir* **15** (1999) 5956.
13. F. M. FOWKES, "Acid-Base Interactions," edited by K. L. Mittal and H. R. Anderson (VPS, Zeist, The Netherlands, 1991).
14. S. T. JOSLIN and F. M. FOWKES, *IEC Prod. R & D* **24** (1985) 369.
15. D. P. ASHTON and R. N. ROTHON, "Controlled Interfaces in Composite Materials," edited by H. Ishida (Elsevier, Amsterdam, 1990).
16. C. M. LIAUW, A. CHILDS, N. S. ALLEN, M. EDGE, K. R. FRANKLIN and D. G. COLLOPY, *Polym. Degrad. Stab.* **63** (1999) 391.
17. R. N. ROTHON, "Particulate Filled Polymer Composites," edited by R. N. ROTHON (Longman Scientific, London, UK, 1996).
18. C. M. LIAUW and S. J. READ, Confidential Report to Cabot Corporation, Billerica, Boston, USA, 1998.
19. C. M. LIAUW, R. N. ROTHON, S. J. HURST and G. C. LEES, *Composite Interfaces* **5** (1998) 503.
20. Cabot North American Technical Report S-136, Cabot Corporation, 1999.
21. H. P. BOEHM, *Carbon* **32** (1994) 759.
22. R. H. BRADLEY, I. SUTHERLAND and E. SHENG, *J. Colloid Interface Sci.* **179** (1996) 561.
23. I. SUTHERLAND, E. SHENG and R. H. BRADLEY, *J. Mater. Sci.* **31** (1996) 5651.
24. J. M. O'REILLY and R. A. MOSHER, *Carbon* **21** (1983) 47.
25. E. PAPIRER and R. LACROIX, *ibid.* **32** (1994) 1341.
26. B. WESSLÉN, M. KOBER, C. FREIJLARSSON, A. LJUNGH and M. PAULSSON, *Biomaterials* **15** (1994) 278.

27. E. ÖSTERBERG and K. BERGSTRÖM, *Appl. Surface Sci.* **64** (1995) 197.
28. T. ASAKAWA, K. OGINO and K. YAMABE, *Bull. Chem. Soc. Japan* **58** (1985) 2009.

29. T. J. FABISH and D. E. SCHLEIFER, *Carbon* **22** (1984) 19.

Received 11 July

and accepted 20 December 2000